### Title
Multifrequency phase and modulation fluorometry.




### Journal
Annual review of biophysics and bioengineering, 13(1)

### ISSN
0084-6589



### Authors
Gratton, E
Jameson, DM
Hall, RD



### Publication Date
1984

### DOI
10.1146/annurev.bb.13.060184.000541

*Ann. Rev. Biophys. Bioeng. 1984. 13: 105–24*

# MULTIFREQUENCY PHASE AND MODULATION FLUOROMETRY[1]

*Enrico Gratton*

Department of Physics, University of Illinois at Urbana-Champaign, Urbana, Illinois 61801

*David M. Jameson*

Department of Pharmacology, The University of Texas Health Science Center at Dallas, Dallas, Texas 75235

*Robert D. Hall*

Laboratory of Molecular Biophysics, National Institute of Environmental Health Sciences, Research Triangle Park, North Carolina 27709

## INTRODUCTION

### *General Aspects*

Determination of characteristic fluorescence parameters i.e. spectral properties, quantum yields, polarizations, and lifetimes, is important in the study of excited states of atoms, molecules, and crystals and also for diagnostic purposes in the physical, chemical, biological, and medical sciences. The appeal of fluorescence methodologies lies in their intrinsic sensitivity and also in the characteristic time scale of the emission process. The excited fluorescent state typically persists for nanoseconds or less, a period that corresponds to the time scale of many important biological

[1] The US Government has the right to retain a nonexclusive, royalty-free license in and to any copyright covering this paper.

processes including diffusion or transport of small molecules over a few angstroms, rotational motions of proteins, internal motions of protein residues, proton transfer reactions, and others. Steady state fluorescence data such as spectra, quantum yields, or polarizations are not always capable of revealing the molecular origins of the observed effects. The correct physical interpretation of many fluorescence experiments requires precise knowledge of the excited state lifetime (59). Moreover, emissions from even simple biological systems will almost always have heterogeneous aspects. This heterogeneity may arise as a consequence of the number and types of fluorophores present or from the complexities of the fluorophore's environment. The characterization of heterogeneous emissions and the assignment of their origins is one of the more challenging problems facing the fluorescence practitioner, and time-resolved measurements offer a powerful means of examining and quantitating these emissions. In this review we describe recent advances of a technique frequently employed for the determination of fluorescence lifetimes and some relevant applications to the biophysical field.

A tremendous effort has been expended during the past twenty years on the development of instrumentation and theory for the measurement and analysis of fluorescence lifetimes. Most of this effort has gone into the development of the impulse response technique, which yields direct recordings of the fluorescence intensity versus time after a brief exciting pulse (1, 58). The harmonic response technique, although practiced in one form or another for more than half a century, has only recently become a popular and powerful alternative to pulse methods. In the traditional harmonic response approach, fluorescence is excited by light with an intensity modulated sinusoidally at high frequencies, typically in the megahertz range. In this case, the fluorescence signal will also be modulated sinusoidally, but the finite persistence of the excited state will lead to a phase delay and demodulation of the fluorescence relative to the excitation (see Figure 1).
provides independent determinations of the fluorescence lifetime (52). The very recent appearance of true multifrequency phase fluorometry has enormously extended the scope and power of the harmonic response technique. In this review we discuss the theoretical basis of multifrequency phase fluorometry, the practical realization of the method, phase and modulation data, and the application of the method to spectroscopic and biochemical problems.

We must clarify at the outset what we mean by multifrequency phase fluorometry. A true multifrequency instrument permits facile selection of arbitrary modulation frequencies over a wide frequency range, e.g. from hundreds of kilohertz to hundreds of megahertz. The aim, however, is to utilize the optimal frequencies for the particular problem in hand. The

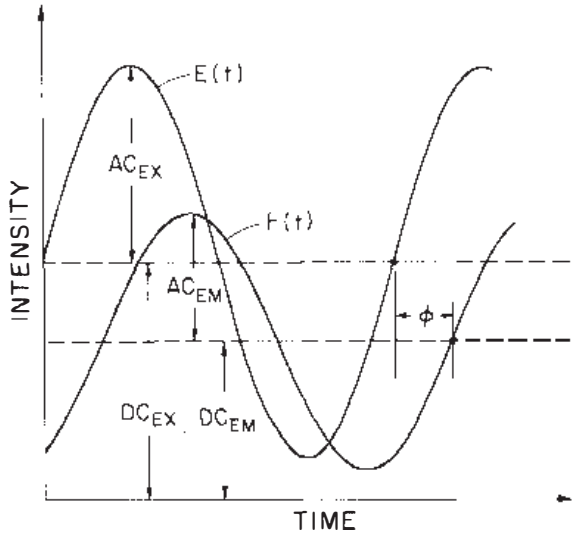


*Figure 1* Schematic representation of the excitation E($t$) and fluorescence F($t$) waveforms. Fluorescence is delayed by an angle $\phi$ and demodulated with respect to excitation.

characteristics of the fluorescence system, i.e. the time scale of the emission process, and not instrumental limitations, should dictate the number and choice of frequencies utilized. The criteria for frequency selection is discussed in detail in a later section.

## BASIC PRINCIPLES

The theory of the phase fluorometer was developed by Dushinsky (11). He demonstrated that a fluorophore characterized by a single exponential decay time $\tau$ will, upon excitation by light with an intensity modulated sinusoidally at an angular frequency, $\omega$, emit light sinusoidally modulated at the same frequency but delayed in phase and demodulated with respect to the excitation (Figure 1). The demodulation is the ratio of the signal amplitude at frequency $\omega$ to the average signal (the AC/DC ratio). The relations between phase shift and modulation ratio and the characteristic time $\tau$ are

$$\phi = \tan(\omega\tau^{P}), \quad M = (1+(\omega\tau^{M})^{2})^{-1/2}, \qquad 1.$$

which provide the basis of two independent determinations of the fluorescence lifetime, i.e. phase ($\tau^{P}$) and modulation ($\tau^{M}$) lifetimes.

If the system described above is replaced by a system of noninteracting fluorophores, each giving rise to a single exponential decay, then a composite sinusoidal emission waveform will result, with a frequency $\omega$ and a phase delay and demodulation given by

$$\phi = \tan^{-1}(S/G), \quad M = (S^{2}+G^{2})^{-1/2}, \qquad 2.$$

where

$$S = \sum_i f_i M_i \sin \phi_i, \quad G = \sum_i f_i M_i \cos \phi_i. \qquad 3.$$

The values of $\phi_i$ and $M_i$ for each component are given by Equation 1; $f_i$ is the fractional intensity of the $i$th component ($\sum_i f_i = 1$). In such a system $\tau^P \neq \tau^M$ and $\tau^P$ and $\tau^M$ are frequency dependent. The functions $S$ and $G$ are the sine and cosine transforms of the impulse response (60). If $I(t)$ represents the free decay after excitation then

$$S = \int_0^\infty I(t) \sin(\omega\tau)dt \Big/ \int_0^\infty I(t)dt,$$

$$G = \int_0^\infty I(t) \cos(\omega\tau)dt \Big/ \int_0^\infty I(t)dt. \qquad 4.$$

These equations provide the basis for the mathematical equivalence between the harmonic and impulse response methods and are useful from the theoretical viewpoint. Certain kinetic decay schemes that are difficult to describe directly in the frequency domain are amenable to time domain formulation. Equation 4 then provides the means to obtain the frequency response of such kinetic schemes. Direct transformation of data between the frequency and time domains is not possible in practice, however, since the actual frequency and time ranges utilized do not extend from zero to infinity, which precludes exact evaluation of the integrals. A critical comparison of practical differences between the two approaches as well as a discussion of the validity of Equation 4 are presented in Reference (28).

# INSTRUMENTATION

## *Brief History*

The development of phase fluorometry has been reviewed in varying detail and from different perspectives several times (e.g. see 6, 28, 53). Phase fluorometers trace their ancestry back to Gaviola's instrument (13), which utilized the Kerr effect to modulate the exciting light and relied upon visual detection of the fluorescence. Some of the important developments in phase fluorometry in the last half century include ultrasonic diffraction grating (39, 52), the use of photomultipliers (46), and measurement of the modulation ratio (4, 21, 52). Many of the early instruments featured direct measurements of the phase delay at the modulation frequency using devices such as oscilloscopes, RC phase compensators, cable delays, and light path compensators (2, 3, 5, 45). Heterodyne techniques permitted the transposition of the signal to the low frequency domain, with subsequent improvement in sensitivity and precision. The advantages of cross-

correlation techniques (discussed in detail later) were demonstrated by Spencer & Weber (52). Early cross-correlation techniques, however, were limited to a few modulation frequencies (49, 52). The modern approach, utilizing a wide and continuously variable frequency range, has realized the full potential of the harmonic method. An excellent account of the development of phase and modulation instrumentation, including the heterodyne and cross-correlation techniques, has been given by Teale (53).

In recent years a renewed interest in phase fluorometry has led to the appearance of a number of instruments (15, 17–19, 25, 38, 47). The more recent instruments differ in their approach to the light modulation principle and the strategy for signal detection and processing, but almost all utilize a CW laser for sample excitation. As we shall see later, synchrotron radiation is also now being utilized for phase and modulation fluorometry. The appearance of commercially available phase and modulation fluorometers, such as the SLM 4800 series, has served to popularize the technique in the biochemical and biophysical fields.

## *Modern Multifrequency Instrumentation*

A multifrequency phase fluorometer using the method of cross-correlation has been recently described (15). Figure 2 shows the layout of this instrument, which was used to obtain much of the data presented in this review. This particular instrument operates over a frequency range of 1 to 160 MHz and gives a time resolution of several picoseconds. The light source is an argon-ion laser and the light modulator is a Pockel's cell. A frequency synthesizer provides the modulated signal to drive the Pockel's

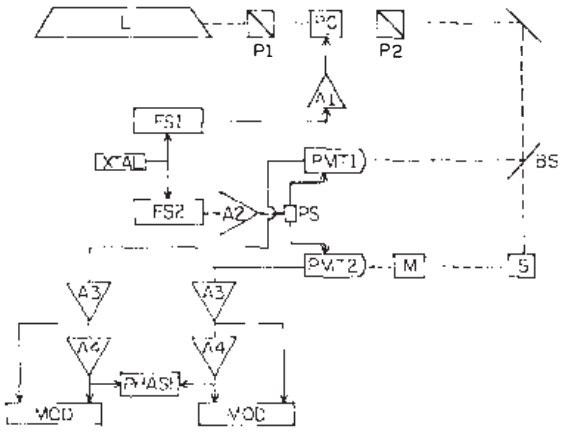


*Figure 2* Block diagram of the laser-based cross-correlation phase fluorometer of Reference (15). L, argon ion laser; A1, 10 W rf power amplifier; A2, 2 W rf power amplifier; XTAL, 10 MHz quartz oscillator; FS1 and FS2, frequency synthesizers; PS, power splitter; PMT1 and PMT2, photomultipliers; M, monochromator; BS, beam splitter; S, sample; A3, pre-amplifier; A4, ac tuned amplifier; PHASE, phase meter; MOD, modulation meter.

cell. A second frequency synthesizer, locked in phase with the first, provides the signal that modulates the photomultiplier's response by varying the voltage at the last dynode. The two synthesizers differ in frequency by a small increment, 31 Hz, which corresponds to the cross-correlation frequency. The optical components are standard; all polarizers are calcite prisms.

In a typical measurement the phase delay and modulation ratio for scattered light (from glycogen or a suspension of latex particles) is determined relative to the signal generated by a reference photomultiplier (see Figure 2) or an internal electronic reference signal. The phase delay and modulation ratio of the fluorescence is then determined relative to the scattered signal (Figure 1). These measurements are repeated at selected modulation frequencies; typical results for fluorophores characterized by single exponential decay and the usual mode of data presentation are shown in Figure 3. Figure 4 shows data for a double exponentially decaying system and the result of a two-component analysis; in this presentation the lifetime values are utilized rather than phase and modulation values. Precision of phase and modulation data is on the order of 0.1° and 2 parts per thousand respectively. Phase and modulation lifetimes are calculated according to Equation 1. Curves corresponding to various decay schemes can be plotted over the data and used to evaluate the fit of the data to a particular scheme.

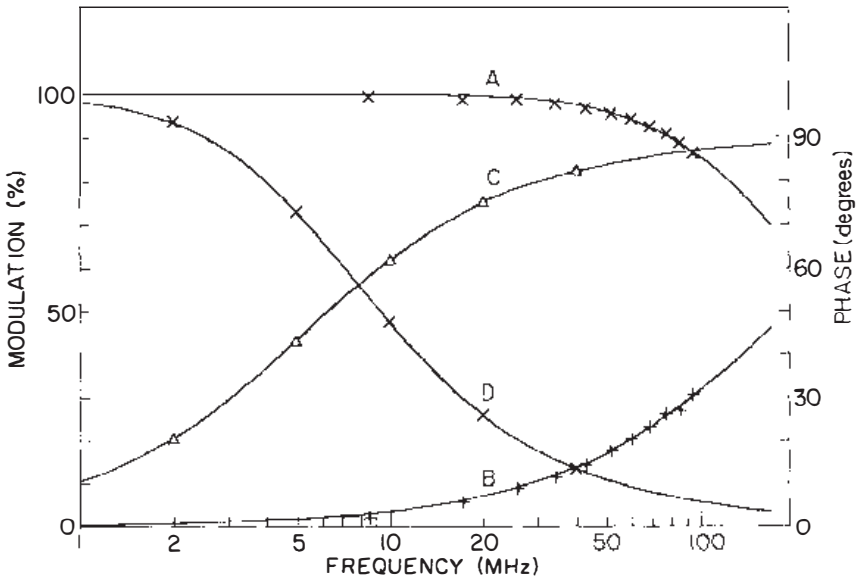


*Figure 3* Multifrequency phase (+,Δ) and modulation (×) data for DENS (2,5-diethylaminonaphthalene sulfonate) in water (curves C and D) and *p*-terphenyl (curves A and B) in cyclohexane. Solid lines correspond to single exponential decays of 29.28 nsec for DENS and 980 psec for *p*-terphenyl.

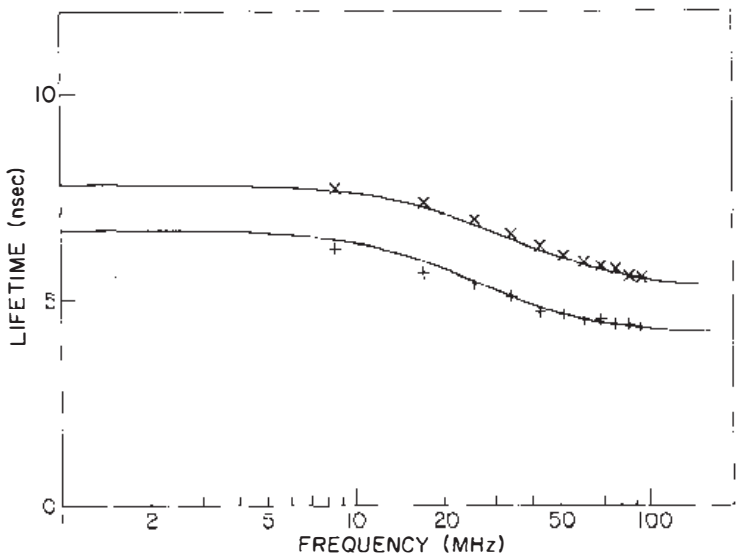


*Figure 4* Multifrequency lifetime data [$\tau^P(+), \tau^M(\times)$] for tryptophan at 20°C, pH 9.25. Solid lines correspond to the best fit using two exponential components $\tau_1 = 3.193 \pm 0.026$ nsec, $\tau_2 = 9.00$ nsec, and $f_1 = 0.396 \pm 0.005$. As noted in the text $\tau^P < \tau^M$ for heterogeneous emission of independent species. Also $\tau^P$ and $\tau^M$ reach constant values at the extremities of the frequency range [see Reference (28) for a discussion of this effect].

## ANALYSIS OF FLUORESCENCE DECAYS

One of the most important features of multifrequency phase and modulation fluorometry is the ability to analyze emission processes other than single exponential decays. Several methods have been proposed for analysis of heterogeneous emissions in terms of the sum of exponential components. Weber obtained the exact solution for the derivation of $N$ exponential lifetime components and their fractional intensities, given phase and modulation data at $N$ modulation frequencies (61). Methods based upon nonlinear least-squares statistical analysis have also been described (27, 28). A critical comparison of the exact and the statistical approaches has revealed that the exact solution requires very high precision in the data and that the uncertainty in the derived parameters increases with the number of measurement frequencies, in contrast to the statistical approach (27). We should emphasize, however, that the exact solution was developed for applications wherein only a few modulation frequencies are available.

Analysis of phase and modulation data has the following two important aspects. We must first recognize which decay schemes are permissible (single exponential, multiexponential, or nonexponential) using well-established statistical methods, based on analysis of the chi-square. Once we adhere to a particular decay scheme, we must evaluate the uncertainty of

the derived parameters and the correlation between these parameters. Also in this case, statistical methods furnish a solution based on analysis of the covariance matrix of the errors associated with the parameters (7).

Coincidence of phase and modulation lifetimes at all modulation frequencies is a necessary and sufficient condition for correct description of a decay as single exponential. Since measured quantities have an associated error, however, and since the frequency range is limited in practice, one cannot rigorously demonstrate the mathematical equivalence of phase and modulation lifetimes but rather must consider this equivalence within the precision of the measurement.

When phase and modulation lifetimes differ, the data must be analyzed according to a more complex scheme, e.g. multiexponential decay. Emitting systems that can properly be described by a double exponential decay include systems composed of two independent emitting species, systems that demonstrate excited state reactions between well-defined states, systems exhibiting energy transfer between two species, isotropic rotators observed through appropriately oriented polarizers, and others. Except for the systems composed of two independently emitting species, the parameters associated with the two-component decay cannot be assigned to particular molecular entities.

Analysis of a double exponential emission gives three independent parameters: two lifetime values and one fractional intensity contribution. We may inquire as to the resolvability of lifetime pairs, given a particular experimental precision and range of modulation frequencies. Our criterion for resolvability is that the derived lifetimes be distinct within their associated errors. Different criteria for resolvability will, of course, lead to different results. The uncertainty in the values of the derived parameters can be determined from the covariance matrix of the errors (discussion of the covariance matrix can be found in any good statistics text; e.g. see 7). In our analysis we assume that the experimental errors in the measured phase and modulation values are independent of modulation frequency [see Reference (15) for a discussion of statistical and systematic errors in phase fluorometry]. In such a case, each term in the covariance matrix has an associated error that becomes a common factor upon evaluation of the matrix. The covariance matrix is then a linear function of the errors associated with the measured phase and modulation values and depends upon the values of the parameters ($\tau_1$, $\tau_2$, and $f_1$) and the frequency set utilized. Furthermore, if the angular modulation frequency range utilized is sufficient to encompass the inverse of the lifetimes of the two components, then the covariance matrix will also be largely independent of the frequency set. The important variables are then the number of frequencies utilized and the values of the parameters. In the case of a double exponential decay with each component

contributing equally to the integrated intensity ($f_1 = f_2$), we can calculate the minimum ratio of the lifetimes that permit resolution of the components. In Figure 5 we report the results of this analysis for a set of eight frequencies (1, 2, 4, 8, 16, 32, 64, and 128 MHz) with errors of $\pm 0.2°$ and $\pm 0.004$ associated with phase and modulation data, respectively. An interesting feature of this analysis is that the width of the nonresolvability zone remains approximately constant from 1 to 500 nsec. Two components (with $f_1 = f_2$) in this lifetime range can be resolved if the ratio of the lifetimes is approximately 1.6. As we have already suggested, the resolvability ratio is proportional to the precision of the measurements.

The method used for the resolvability analysis has general applicability, and other cases with $f_1 \neq f_2$ can be readily evaluated. In Figure 6 we analyze the dependence of the resolvability ratio on the number of frequencies utilized. The errors on the parameters are proportional to the reciprocal of a fractional power (ranging from 1/2 to 1/3 in all cases studied) of the number of frequencies. This analysis demonstrates that decreasing the errors in the parameters by a factor of two (to subsequently improve the resolvability ratio twofold) requires that the number of modulation frequencies be increased by a factor ranging from 4 to 8. The use of a large number of modulation frequencies is impractical and unnecessary and, except for special applications, 3 to 10 frequencies scaled logarithmically in the range of 1 to 200 MHz suffice for practical purposes. A frequency set such as 1, 2, 4, 8, 16, 32, 64, 128, and 256 MHz is ideal.

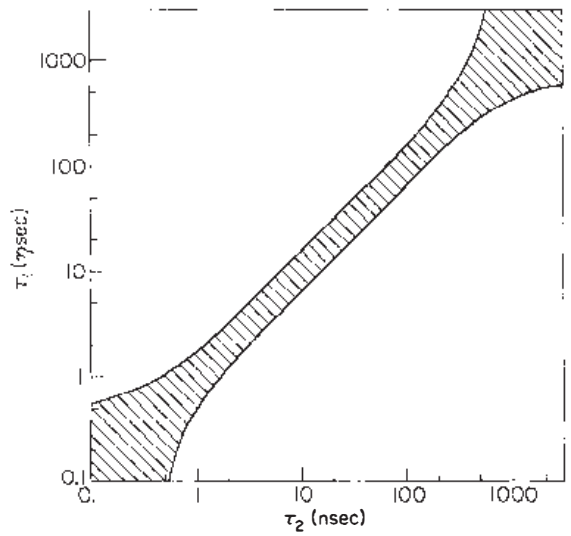


*Figure 5* Double exponential decay resolvability plot. Lifetime pairs $\tau_1$ and $\tau_2 (f_1 = f_2)$ in the shaded region cannot be resolved using the frequency set 1, 2, 4, 8, 16, 32, 64, and 128 MHz if the precision of phase and modulation measurements is $>0.2°$ and $>0.004$ respectively.

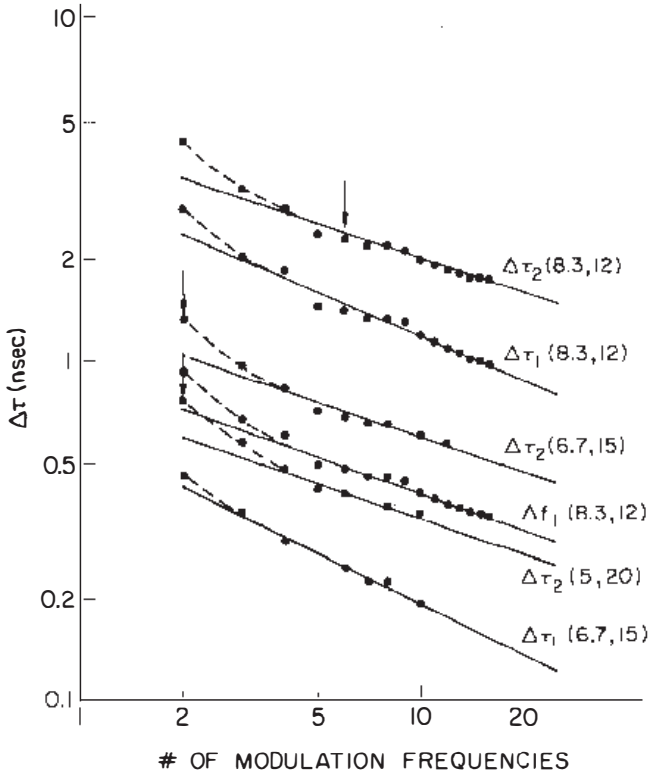


*Figure 6* Double exponential decay lifetime and fractional intensity uncertainties as a function of the number of frequencies utilized for the measurements. In parentheses selected pairs of lifetime in nanoseconds ($f_1 = f_2$). Arrows indicate the minimum number of frequencies needed. Frequencies are chosen equally spaced on a log scale in the range 1 to 256 MHz.

In some cases of two independently emitting species, the lifetimes of the two components may be known already and the fractional contributions may be the unknown quantities. In such cases, analysis of the covariance matrix of the errors, similar to that performed for the previous case, demonstrates the possibility of obtaining the fractional contributions with high precision (0.7–0.8% error), using a single modulation frequency. The optimum modulation frequency is that which corresponds to the average (in the log scale) of the frequencies given by the inverse of the two lifetimes. Figure 7 shows the error on the fractional intensity as a function of the modulation frequency for a given lifetime pair. This analysis is pertinent to the consideration of the optimum modulation frequency for use with phase-sensitive detection techniques (discussed later). The small error on the fractional intensities justifies the use of a single modulation frequency to obtain phase-resolved spectra of individual components in a mixture when the two lifetimes are given.

Having outlined the general rules for resolvability of a double exponen-

tial decay, we may now consider the application of multifrequency phase and modulation data to other emission decay schemes.

1. The emission from a system undergoing an excited state reaction between two well-defined states will be double exponential, but the two lifetime values cannot be assigned to either of the reacting species. Such a system can be described by six parameters: two radiative decay rates for each molecular species, the forward and reverse reaction rates, the ratio of extinction coefficients of each species at excitation wavelength, and the ratio of fluorescence intensities of each species at emission wavelength. Since analysis of a double exponential decay yields only three independent parameters, the system cannot be analyzed in the absence of simplifying considerations. Simplification is often possible, however, through judicious choice of excitation and emission wavelengths to minimize the contribution of one species. Also, in many cases some of the rates are quite large compared to others. Hence, the number of parameters can often be reduced and the system fully determined. The form of the equations, applicable in phase fluorometry, for excited state reactions has been given (34) and can also be obtained from the impulse response using Equation 4. Systems that fall in the general category of excited state reactions include collisional quenching of the fluorescence, energy transfer reactions, excimer formation, and proton transfer reactions.

2. Measurements on the decay of emission anisotropy will yield a double exponential decay for the case of an isotropic rotator and for some other rotational modes as well (60). The harmonic response of these systems

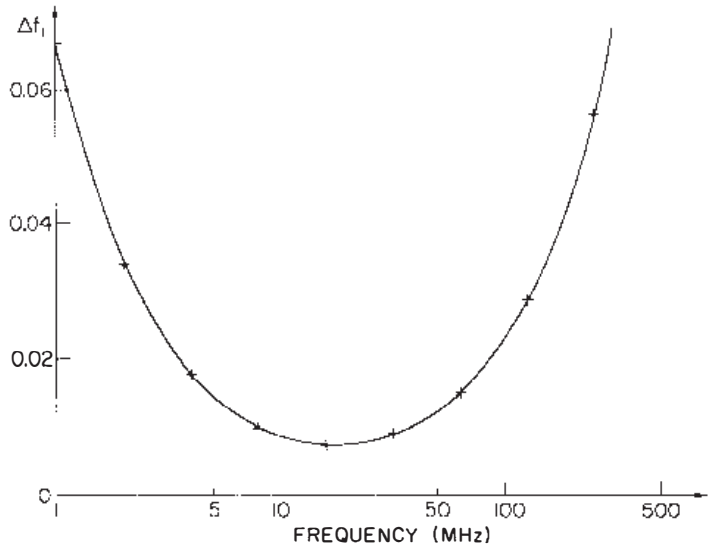


*Figure 7* Frequency dependence of fractional intensity uncertainty for a double exponential decay ($\tau_1 = 6.7$ nsec, $\tau_2 = 15$ nsec, and $f_1 = 0.5$).

can be derived from the impulse response through the application of Equation 4.

## *Differential Methods*

Phase and modulation fluorometry is inherently a differential technique, since the phase delay and modulation ratio of the emission is measured relative to a reference. In some cases a convenient choice of the reference can simplify the analysis and improve the precision of the measurement. We have pointed out that in the case of an interconverting system the decay rate is a property of the system rather than corresponding to particular molecular entities. If one can isolate the emission from each species of interest, for example by proper selection of the excitation or emission wavelengths or appropriately oriented polarizers, then the phase delay between the two species, and their relative modulation ratios, can be directly determined. Weber (60) has derived general expressions for the differential tangent and modulation ratio corresponding to two emissions, each of which is represented by a sum of exponentials:

$$\Delta = \tan(\phi_2 - \phi_1), \quad Y = M_2/M_1, \tag{5.}$$

where $\phi_1, M_1$, and $\phi_2, M_2$ are the phase delay and modulation ratio of the emission from molecular species 1 and 2 respectively and are given by expressions such as Equation 2.

1. For the case of two independent species one finds

$$\Delta = \omega(\tau_2 - \tau_1)/(1 + \omega^2\tau_1\tau_2), \quad Y^2 = [1 + (\omega\tau_1)^2]/[1 + (\omega\tau_2)^2]. \tag{6.}$$

These expressions are often used when the phase and modulation of a sample are measured relative to a fluorescence reference signal in place of a scatter solution in order to minimize certain systematic errors such as wavelength-related time response of the photomultiplier. The shape of the differential tangent versus frequency curve corresponds to a Lorentzian with a maximum:

$$\omega^2_{\max} = 1/(\tau_1\tau_2). \tag{7.}$$

2. For the case of the parallel and perpendicular components of the emission from an isotropic rotator, excited with parallel polarized light, one obtains

$$\begin{aligned} \Delta &= (3\omega r R)/[(k^2 + \omega^2)(1 + r - 2r^2) + R(R + 2k + kr)], \\ Y^2 &= \{[k + 6R/(1 - r)]^2 + \omega^2\}/\{[k + 6R/(1 + 2r)]^2 + \omega^2\}, \end{aligned} \tag{8.}$$

where $r$ is the limiting anisotropy, $R$ the rotational rate, and $k$ the radiative decay rate.

In this case also, the differential tangent versus frequency curve is a Lorentzian with a maximum given by

$$\omega_{max}^2 = k^2 + R(R+2k+kr)/(1+r-2r^2). \quad 9.$$

For anisotropic rotators, the frequency dependence of the differential tangent curve has maxima corresponding to each individual rotation rate, and the absolute value of each maximum is less than that corresponding to an isotropic rotator, a difference termed the tangent defect (60). Examples of isotropic and more complex rotations are given in the applications section.

3. For the case of an interconverting system (e.g. excited state deprotonation or energy transfer) in which the back reaction rate is negligible (and only the initial species is directly excited), the differential tangent and modulation ratio have a simple expression:

$$\Delta = \omega\tau_2, \quad Y = [1+(\omega\tau_2)^2]^{-1/2}. \quad 10.$$

In this particular case, differential methods permit us to obtain the forward reaction rate independently of the radiative decay rate (34).

## APPLICATIONS

### *Noninteracting Systems Characterized By Double Exponential Decays*

The analysis of double exponential decays for the component lifetimes and their fractional contributions may proceed with two general goals in mind. The first goal may be a characterization of the nature and extent of the heterogeneity, with the aim, for example, of studying the molecular photophysics of a fluorophore, determining distribution of fluorophores in different environments, or achieving a compositional description of a system. The second goal may be utilization of the heterogeneity as a tool in the analysis of the dynamics of equilibria of complex systems. An example of the latter case would be a titration experiment to determine the extent of binding in a protein-ligand system.

Phase and modulation lifetime heterogeneity studies have been carried out on a number of systems including membranes (30, 41) and various protein systems (10, 12, 22, 24, 44, 48, 50, 51, 57). A study of the pH-dependent heterogeneity of tryptophan (29) was carried out with the aim of evaluating Weber's exact solution. A recent review discusses a number of these studies (28).

### *Excited State Reactions*

Several types of excited state reactions have been investigated, using phase fluorometry, with the aim of obtaining information on the reaction rates as

well as spectral properties. For example, quenching of fluorescence by small molecules such as oxygen and acrylamide has been extensively studied. In particular, quenching of the tryptophan fluorescence of a number of globular proteins was studied by phase fluorometry (37). In these studies, however, only a single modulation frequency was utilized and only phase data were obtained. Lifetime results were important in establishing the dynamic character of quenching but could not be used to analyze the details of the quenching process. A detailed multifrequency phase and modulation study on oxygen quenching of the prophyrin emission of iron-free myoglobin and hemoglobin was recently reported (26). The results were interpreted in terms of a general model for dynamic quenching of the fluorescence of globular proteins, which, in the limit of low oxygen concentrations, yields double exponential decay. The multifrequency data permitted assignment of the rate of acquisition of quencher by the protein, the exit rate of quencher from the protein, and the migration rate of quencher in the protein interior.

## *Dipolar Relaxations*

A complete theory to account for the dynamics of dipolar relaxations in pure solvents and complex environments such as protein interiors has not yet appeared. The information we seek from dipolar relaxation studies concerns the modalities of the relaxation of the initial Frank-Condon state. A multistate or continuous model is required to describe the phenomenon accurately. However, theoretical difficulties in elaborating a continuous model have led many researchers to adopt the simpler phenomenological approach of considering only an initial unrelaxed and a final relaxed state (33, 62). In this case the general framework of a double exponential decay can be applied. In Figure 8 we report the result of this type of analysis for dansylaziridine derivative [S-(dansyl aminoethyl)-2-thioethanol] in propylene glycol at $-42°C$. The results of a double exponential analysis indicate that the decay rates change in a continuous fashion across the emission spectrum and that the fractional intensity of one component increases to a value greater than unity towards the red (note that for a relaxing system the value of a fractional intensity may exceed unity). For a two-state system, however, the values of the fractional intensities must become constant at the two extremities of the spectrum, and the decay rates of the two components must be wavelength independent. The dansylaziridine derivative results thus demonstrate the inadequacy of the simple two-state approach.

Spectral relaxation studies are often presented in the form of time-resolved spectra, i.e. the emission spectra at selected times after the exciting light pulse. Multifrequency phase fluorometry can also be utilized to obtain time-resolved spectra as shown in Figure 9 for TNS (*p*-2-toluidinyl-6-

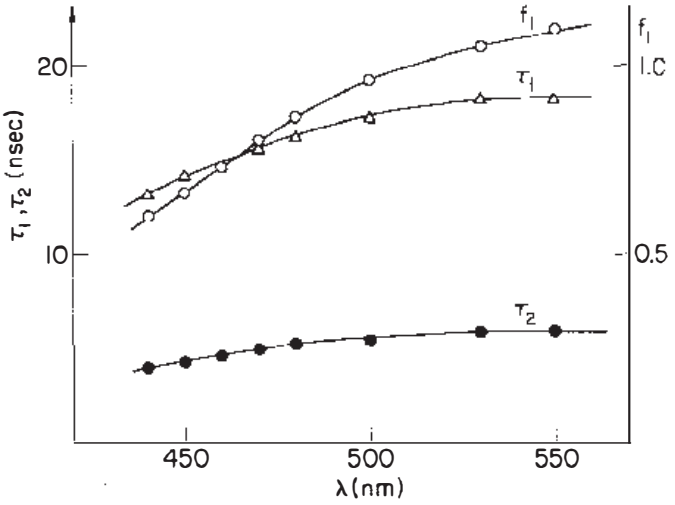


*Figure 8* Double exponential decay analysis of dansylaziridine derivative in propylene glycol at −42°C.

naphthalene sulfonic acid) in glycerol (14). Although this example shows the capabilities of multifrequency phase fluorometry to accurately record the characteristics of the emission of relaxing systems, a more complete theoretical treatment of solvent relaxation processes is required for rigorous data analysis.

## *Rotations*

Expressions for the differential tangent and ratio of modulations for isotropic and anisotropic rotators were derived by Weber (60). Mantulin & Weber (40) performed a number of differential phase measurements at two

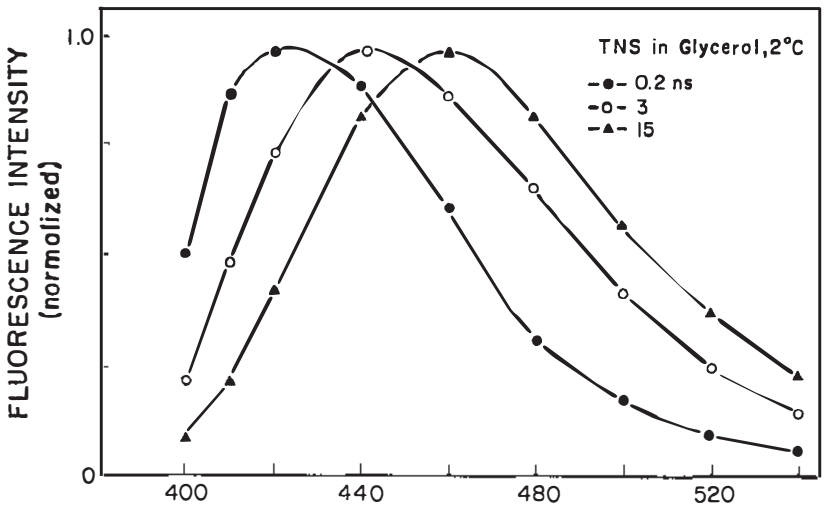


*Figure 9* Time-resolved spectra of TNS in glycerol.

modulation frequencies on a series of unsubstituted aromatic hydrocarbons (anthracene, perylene, and chrysene) as well as fluorophores capable of forming hydrogen bonds with the solvent, propylene glycol. In these studies the rotational rates were altered by changing the temperature, and hence the viscosity, of the solvent. The results indicated strongly anisotropic rotations for the unsubstituted fluorophores and isotropic rotations for those fluorophores capable of forming two or more hydrogen bonds. These investigations inspired a number of differential phase studies on fluorophore rotations in model and natural membrane systems (8, 9, 36).

Multifrequency phase and modulation fluorometry was used extensively by Hauser and co-workers for investigations of rotation of small molecules in pure solvents (20, 31, 32). Rotational diffusion times for oxypyrene trisulfonate, rhodamine 6G, and perylene in water were measured; only isotropic rotations were discernible. The phase fluorometer utilized was operational at frequencies up to 400 MHz, and rotational diffusion rates of a few tenths of picoseconds were measurable representing the shortest rotational times directly observed using phase fluorometry.

Figure 10 presents some recent results (Eccleston, Jameson, and Gratton, unpublished observations) on the differential tangent of a fluorescent derivative of GDP (2′-amino-2′-deoxy GDP derivatized on the 2′ amino group with fluorescamine) free in solution and bound to elongation factor

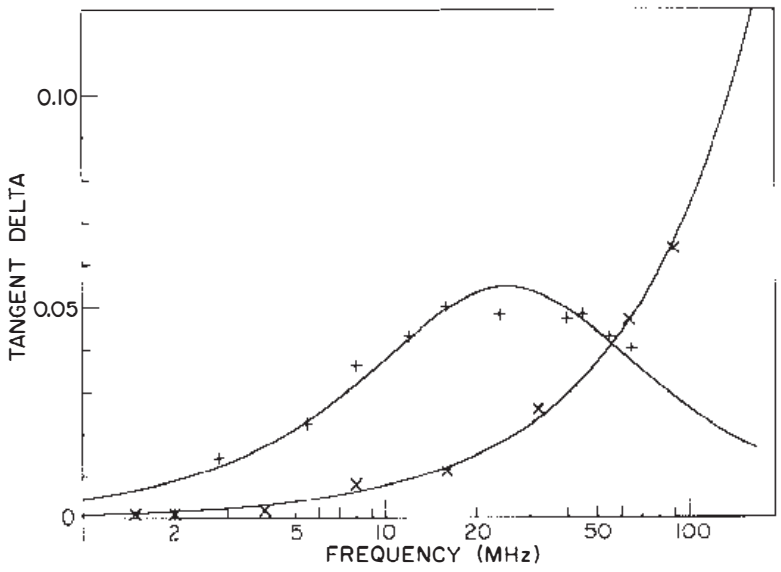


*Figure 10* Polarized differential tangent plot for fluoram-GDP free (×) and bound (+) to elongation factor TU from *E. coli*. Excitation wavelength 351 nm, emission wavelength >460 nm. Solid lines correspond to rotational rate of 68 nsec and limiting anisotropy 0.08 for the bound species and rotational rate of 0.15 nsec and limiting anisotropy of 0.35 for the free species.

Tu from *Escherichia coli.*
was used to obtain data over the frequency range of 1 to 100 MHz. The bound fluorophore gave the characteristic bell-shaped curve peaking at intermediate frequencies while the curve corresponding to free fluorophore (resulting from displacement of the probe from the protein by the addition of excess GDP) was shifted to higher frequencies. We should note that a multifrequency analysis on the emission of the free and bound probe indicated a single exponential decay in each case with lifetimes of 7.70 and 11.03 nsec respectively. This application demonstrates that multifrequency measurements at a single temperature and viscosity can yield rotational rates and limiting anisotropies; the information content is thus the same as that from decay of anisotropy experiments carried out using pulse techniques.

## *Phase-Sensitive Detection*

Phase-sensitive detection has been a standard methodology in fluorometry for many years (6, 28, 53). Veselova et al, however, first applied the technique to resolve individual intensity components of heterogeneous emissions from simple fluorescence solutions (54–56). The basic idea of phase-sensitive detection is that emissions corresponding to two species can be individually recorded upon illumination of the system with light modulated at an appropriate frequency if the species differ in lifetime and if the emission is viewed with a detector sensitive to the phase delay. Two conditions render phase-sensitive detection feasible: first, the total intensity of a sinusoidally modulated fluorescence signal is the sum of the intensity components of the individual emitting species; second, the amplitude of the phase-detected signal depends upon both the phase angle of detection and the phase angles of the individual components relative to a reference signal of the same frequency. These considerations are expressed in the relationship (28)

$$PSD = \sum_i I_i(\lambda) f_i M_i \cos(\phi_i - \phi_D), \qquad 11.$$

where $I_i(\lambda)$ is the relative intensity as a function of wavelength, $f_i$ is the fractional intensity contribution, $M_i$ is the modulation, $\phi_i$ the phase angle of the $i$th species, and $\phi_D$ the phase angle of the detector. Clearly, setting $\phi_D = \phi_i \pm 90°$ eliminates the fluorescence of the $i$th species. Selection of the appropriate modulation frequency for phase sensitive detection has been discussed in the analysis section.

Phase-sensitive detection has been applied to several systems relevant to the spectroscopy of proteins such as mixtures of tyrosine and tryptophan (35, 42) and human serum albumin in which the tyrosine contribution was isolated. The resolution of anthracene-diethylaniline exciplex emission (35)

illustrated the acquisition of spectra at different detector phase angles. The effect of dipolar relaxation upon phase-resolved spectra has been investigated using *n*-acetyl-L-tryptophanamide in propylene glycol (33); a simple method for estimating spectral relaxation times from phase sensitive intensities was given. The effect of modulation frequency upon the resolving power of the phase-sensitive technique was recently illustrated (42).

## CONCLUSIONS AND FUTURE PROSPECTS

In the last few years, multifrequency phase and modulation fluorometry has developed into a powerful technique for the examination of excited state processes. Processes amenable to analysis include heterogeneous emissions, excited state reactions, dipolar relaxations, and rotational motions. Multifrequency instruments generally utilize sinusoidal modulation of continuous light sources. Intrinsically modulated sources such as synchrotron radiation and mode-locked lasers may, however, be utilized to collect phase and modulation data (16, 44). For example, the data in Figure 3 on *p*-terphenyl and in Figure 4 on tryptophan were obtained with a multifrequency apparatus utilizing synchrotron radiation at the ADONE storage ring in Frascati, Italy. The instrumentation used in these studies is virtually identical to that described in Reference (15), with the exception of the modulated light source; the frequencies utilized represent the harmonics of the fundamental ring frequency (8.568 MHz at ADONE). Note that one cannot distinguish between measurements done with a pulsed source and those utilizing sinusoidal light modulation. The extensive wavelength range available from synchrotron radiation is a particularly advantageous feature, as is the fact that all wavelengths are rigorously simultaneous. High repetition rate pulsed sources are ideal for multifrequency phase and modulation measurements, since the harmonic content of such sources extends to very high frequencies. The availability of very high modulation frequencies (in the gigahertz range) would permit complete characterization of rotational modes of small molecules in fluid solvents. Such rotational studies would also be extremely useful in investigation of rotations of tyrosine and tryptophan residues in proteins; molecular dynamics calculations predict very fast rotations, on the picosecond time scale, for some of these residues (23, 43).

Since data acquisition and analysis in phase fluorometry is rapid (compared to the more commonly utilized pulse techniques), one may in principle perform kinetic lifetime studies on systems with rate constants in the range of seconds or less. One may also envision the use of multifrequency techniques in analytical applications such as quantitation of sample purity.

Finally, we may speculate that multifrequency phase and modulation fluorometry could eventually prove to be an important diagnostic technique in cell biology and clinical chemistry. Lifetime measurements offer distinct advantages over intensity and even polarization data in that the contributions from various components (scattered light, for example) can often be unequivocally assigned. The requisite instrumentation is no longer a laboratory curiosity but is, in fact, easy to operate and readily accessible to researchers in diverse fields.

## ACKNOWLEDGMENTS

Sincere and grateful appreciation is expressed to G. Weber for his support and encouragement of the development of multifrequency phase fluorometry. We are indebted to M. Limkeman for statistical analysis. Research in our lab (E.G.) is supported by Grants PCM79-18646 and ICR-Physics 1-2-22190.

*Literature Cited*

1. Badea, M. G., Brand, L. 1979. *Methods Enzymol.* 61:378–425
2. Bailey, E. A., Rollefson, G. K. 1953. *J. Chem. Phys.* 21:1315–22
3. Bauer, R., Rozwadowski, M. 1959. *Bull. Acad. Pol. Sci. Ser. Sci. Math. Astron. Phys.* 7:365–68
4. Birks, J. B., Dyson, D. J. 1961. *J. Sci. Instrum.* 38:282–85
5. Birks, J. B., Little, W. A. 1953. *Proc. Phys. Soc. London Sect. A* 66:921–28
6. Birks, J. B., Munro, I. H. 1967. *Prog. React. Kinet.* 4:239–303
7. Brandt, S. 1976. *Statistical and Computational Methods in Data Analysis.* Amsterdam: North-Holland. 2nd ed.
8. Chong, P., Cossins, A. R. 1983. *Biochemistry* 22:409–15
9. Cossins, A. R., Kent, J., Proffer, C. L. 1908. *Biochim. Biophys. Acta* 599:341–58
10. Dalbey, R. E., Weiel, J., Yount, R. G. 1983. *Biochemistry* 22:4696–4706
11. Dushinsky, F. 1933. *Z. Phys.* 81:7–21
12. Eftink, M. R., Jameson, D. M. 1982. *Biochemistry* 21:4443–49
13. Gaviola, E. 1926. *Ann. Phys. Leipzig* 81:681–710
14. Gratton, E., Lakowicz, J. R. 1983. Presented at Ann. Meet. Am. Soc. Photobiol., 11th, Madison, Wis.
15. Gratton, E., Limkeman, M. 1983. *Biophys. J.* In press
16. Gratton, E., Lopez-Delgado, R. 1980. *Nuovo Cimento B* 56:110–24
17. Gugger, H., Calzaferri, G. 1980. *J. Photochem.* 13:21–33
18. Gugger, H., Calzaferri, G. 1980. *J. Photochem.* 13:295–307
19. Haar, H. P., Hauser, M. 1978. *Rev. Sci. Instrum.* 49:632–33
20. Haar, H. P., Klein, U. K. A., Hafner, F. W., Hauser, M. 1977. *Chem. Phys. Lett.* 49:563–67
21. Hamilton, T. D. S. 1957. *Proc. Phys. Soc. London Sect. B* 70:144–45
22. Herron, J., Voss, E. W. 1981. *J. Biochem. Biophys. Methods* 5:1–17
23. Ichiye, T., Karplus, M. 1983. *Biochemistry* 22:2884–93
24. Ide, G., Engelborghs, Y. 1983. *J. Biol. Chem.* 256:11684–87
25. Ide, G. Engelborghs, Y., Persoons, A. 1983. *Rev. Sci. Instrum.* 54:841–44
26. Jameson, D. M., Alpert, B., Gratton, E., Weber, G. 1983. *Biophys. J.* In press
27. Jameson, D. M., Gratton, E. 1983. In *New Directions in Molecular Luminescence*, ed. D. Eastwood, L. Cline-Love, pp. 67–81. Philadelphia: ASTM.
28. Jameson, D. M., Gratton, E., Hall, R. D. 1983. *Appl. Spectrosc. Rev.* 20: In press
29. Jameson, D. M., Weber, G. 1981. *J. Phys. Chem.* 85:953–58
30. Klausner, R. D., Kleinfeld, A. M., Hoover, R. L., Karnovsky, M. J. 1980. *J. Biol. Chem.* 255:1286–95
31. Klein, U. K. A., Haar, H. P. 1978. *Chem. Phys. Lett.* 58:531–35

32. Klein, U. K. A., Haar, H. P. 1979. *Chem. Phys. Lett.* 63:40–42
33. Lakowicz, J. R., Balter, A. 1982. *Photochem. Photobiol.* 36:125–32
34. Lakowicz, J. R., Balter, A. 1982. *Biophys. Chem.* 16:99–115
35. Lakowicz, J. R., Cherek, H. 1981. *J. Biochem. Biophys. Methods* 5:19–35
36. Lakowicz, J. R., Prendergast, F. G., Hogen, D. 1979. *Biochemistry* 18:508–19
37. Lakowicz, J. R., Weber, G. 1973. *Biochemistry* 12:4171–79
38. Lytle, F. E., Pelletier, M. J., Harris, T. D. 1979. *Appl. Spectrosc.* 33:28–32
39. Maercks, O. 1938. *Z. Phys.* 109:685–99
40. Mantulin, W. W., Weber, G. 1977. *J. Chem. Phys.* 66:4092–99
41. Matayoshi, E. D., Kleinfeld, A. M. 1981. *Biophys. J.* 35:215–35
42. Matheis, J. R., Mitchell, G. W., Spencer, R. D. 1983. See Ref. 27. In press
43. McCammon, J. A., Wolynes, P. G., Karplus, M. 1979. *Biochemistry* 18:927–42
44. Moya, I., Garcia, R. 1983. *Biochim. Biophys. Acta* 722:480–91
45. Muller, A., Lumry, R., Kokubun, H. 1965. *Rev. Sci. Instrum.* 36:1214–26
46. Ravilious, C. F., Farrar, R. T., Liebson, S. H. 1954. *J. Opt. Soc. Am.* 44:238–41
47. Saleem, I., Rimai, L. 1977. *Biophys. J.* 20:335–42
48. Sarkar, H. K., Song, P.-S., Leong, T.-Y., Briggs, W. R. 1982. *Photochem. Photobiol.* 35:593–95
49. Schmillen, A. 1953. *Z. Phys.* 135:294–308
50. Schuldiner, S., Spencer, R. D., Weber, G., Weil, R., Kaback, H. R. 1975. *J. Biol. Chem.* 250:8893–98
51. Sebban, P., Moya, I. 1983. *Biochim. Biophys. Acta* 722:436–42
52. Spencer, R. D., Weber, G. 1969. *Ann. NY Acad. Sci.* 158:361–76
53. Teale, F. W. J. 1983. In *Time Resolved Fluorescence Spectroscopy in Biochemistry and Biology*, ed. E. B. Cundall, R. E. Dale, *NATO ASI, Life Sci. Ser. A* 69:59–80. London: Plenum
54. Veselova, T. V., Cherkasov, A. S., Shirokov, V. I. 1970. *Opt. Spectrosc. USSR* 29:617–18
55. Veselova, T. V., Limareva, L. A., Cherkasov, A. S. 1965. *Izv. Akad. Nauk. SSSR, Bull. Phys. Ser.* 29:1345–54
56. Veselova, T. V., Shirokov, V. I. 1972. *Izv. Akad. Nauk. SSSR, Bull. Phys. Ser.* 36:925–28
57. Visser, A. J. W. G., Grande, H. J., Veeger, C. 1980. *Biophys. Chem.* 12:35–49
58. Ware, W. R. 1971. In *Creation and Detection of the Excited State*, ed. A. A. Lamola, 1A:213–302. New York: Dekker
59. Weber, G. 1976. *Horizon Biochem. Biophys.* 2:163–98
60. Weber, G. 1977. *J. Chem. Phys.* 66:4081–91
61. Weber, G. 1981. *J. Phys. Chem.* 85:949–53
62. Weber, G., Mitchell, G. W. 1976. In *Excited States of Biological Molecules*, ed. J. B. Birks. New York: Wiley

*Annual Review of Biophysics and Bioengineering*
*Volume 13, 1984*

# CONTENTS



 (*continued*)